Signatures of spinning evaporating micro black holes

Antonino Flachi, Misao Sasaki, Takahiro Tanaka

Yukawa Institute for Theoretical Physics, Kyoto University, Kyoto 606–8502, Japan

Abstract

We consider the evaporation of rotating micro black holes produced in highly energetic particle collisions, taking into account the polarization due to the coupling between the spin of the emitted particles and the angular momentum of the black hole. The effect of rotation shows up in the helicity dependent angular distribution significantly. By using this effect, there is a possibility to determine the axis of rotation for each black hole formed, suggesting a way to improve the statistics. Deviation from thermal spectrum is also a signature of rotation. This deviation is due to the fact that rapidly rotating holes have an effective temperature $T_{\rm eff}$ significantly higher than the Hawking temperature T_H. The deformation of the spectral shape becomes evident only for very rapidly rotating cases. We show that, since the spectrum follows a blackbody profile with an effective temperature, it is difficult to determine both the number of extra-dimensions and the rotation parameter from the energy spectrum alone. We argue that the helicity dependent angular distribution may provide a way to resolve this degeneracy. We illustrate the above results for the case of fermions.

In this paper, we consider micro black holes resulting from the collision of two particles at energies much higher than the higher dimensional Planck mass M_P [1, 2, 3, 4]. We have in mind models with M_P of order of a few TeV and the standard model confined on a 3-brane, embedded in a $(4+n)$-dimensional bulk [5, 6]. These black holes have horizon radius smaller than the size of the extra dimensions, and are expected to follow balding, spin-down, Schwarzschild, and Planck phases. Micro black hole formation has been studied both analytically [7] and numerically [8], and their evaporation has also been the subject of considerable attention (see for example [9, 10]). Previous work suggests that micro black holes mostly evaporate into brane modes [12].

We analyze the fermion emission from spinning evaporating micro black holes, whose geometry can be approximated by a vacuum higher dimensional Kerr [13]:

$$\begin{aligned} ds^2 &= \left(1-\frac{M}{\Sigma r^{n-1}}\right)dt^2+\frac{2aM\sin^2\theta}{\Sigma r^{n-1}}dtd\varphi-\frac{\Sigma}{\Delta}dr^2-\Sigma d\theta^2-\left(r^2+a^2+\frac{a^2M\sin^2\theta}{\Sigma r^{n-1}}\right)\sin^2\theta d\varphi^2 \\ &\quad -r^2\cos^2\theta d\Omega_n^2 \ , \end{aligned}$$

where $\Delta\equiv r^2+a^2-Mr^{1-n}$ and $\Sigma\equiv r^2+a^2\cos^2\theta$. M_P is normalized to one. Since we are interested in the visible brane modes, the background spacetime will be given by the projection of the above metric on the brane. Massless fermions emitted by the black hole are described by the Dirac equation:

$$e^\mu_a\gamma^a\left(\partial_\mu+\Gamma_\mu\right)\psi=0 \ ,$$

where ψ is the Dirac spinor wave function, e^μ_a a set of tetrads, Γ_μ the spin-affine connections determined by $\Gamma_\mu=\gamma^a\gamma^b\omega_{ab\mu}/4$, with $\omega_{ab\mu}$ being the Ricci rotation coefficients. The matrices $\gamma^\mu=e^\mu_a\gamma^a$ are chosen to satisfy the relation $\gamma^\mu\gamma^\nu+\gamma^\nu\gamma^\mu=g^{\mu\nu}$, with $g^{\mu\nu}$ being the metric on the brane.

Due to the symmetries of the Kerr spacetime, the spinor wave function factorizes as [14]

$$\psi=\mathcal{N}e^{i(m\varphi-\omega t)}\left(\begin{array}{c}\vec{\phi}\\ \pm\vec{\phi}\end{array}\right) \ ,$$

where the + and − signs refer to negative and positive helicities, respectively. We illustrate the results for the case of negative helicity. The positive helicity case can be obtained by a trivial chirality transformation. The field $\vec{\phi}$ takes the form

$$\vec{\phi}=\left(\begin{array}{c}R_-(r)S_-(\theta)\\ R_+(r)S_+(\theta)\end{array}\right) \ ,$$

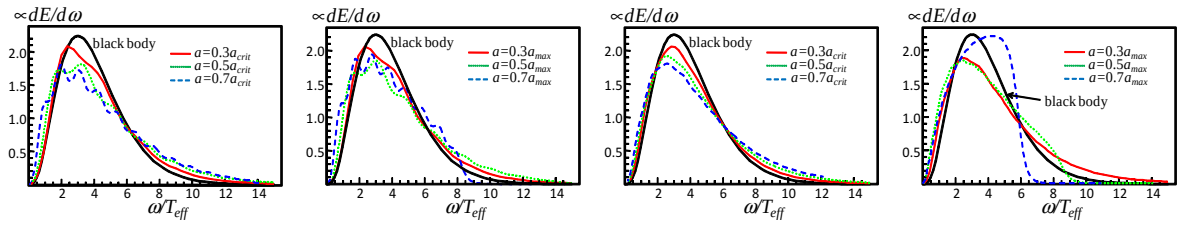

Figure 1: Energy spectrum of the emitted fermions. The horizontal axis is rescaled by the effective temperature determined by fitting the data by a black body profile. The overall amplitude is normalized since the absolute magnitude is not observable. The first (last) two panels from left refer to $n = 2$ ($n = 4$).

and the normalization factor is $\mathcal{N}^{-1} = \Delta^{1/4}(r + ia\cos\theta)^{1/2}\sin^{1/2}\theta$. The angular and radial modes obey

$$\left(\frac{d}{d\theta} \pm \omega a \sin\theta \mp \frac{m}{\sin\theta}\right) S_{\mp}(\theta) = \pm\kappa S_{\pm}(\theta) \ ,$$
$$\left(\frac{d}{dr} \mp \frac{i}{\Delta}\left(\omega(r^2+a^2) - ma\right)\right) R_{\mp}(r) = \kappa\Delta^{-1/2} R_{\pm}(r) \ ,$$

where κ is a separation constant. Supplemented with regularity conditions at $\theta = 0$ and π, the set of angular equations provides an eigenvalue problem, which determines κ [16]. In order to compute the particle flux, we impose ingoing boundary conditions at the horizon. The number of (negative helicity) particles emitted, for fixed frequency ω, is distributed according to the Hawking radiation formula:

$$\frac{dN}{d\omega d\cos\theta} = \frac{1}{2\pi\sin\theta}\sum_{l,m} |S_-(\theta)|^2 \frac{\sigma_{l,m}}{e^{\tilde{\omega}/T_H}+1} \ , \tag{1}$$

where $\tilde{\omega} = \omega - ma/(r_h^2+a^2)$, $T_H = \frac{1}{4\pi r_h}\frac{(n+1)r_h^2+(n-1)a^2}{r_h^2+a^2}$ is the Hawking temperature, and $\sigma_{l,m}$ the grey-body factor (see Ref. [17]). The initial angular momentum of the produced black holes $J = 2aM/(n+2)$ is restricted by requiring the impact parameter $b = J/M$ to be smaller than the horizon radius r_h, determined by $\Delta(r_h) = 0$. Then, the maximum value of the rotation parameter a turns out to be $a_{max} = \frac{n+2}{2} r_h$ [9]. The upper bound on J might be even lower for $n \geq 2$. In fact, there exists a critical value for a, $a_{crit} \equiv (n+1)(n-1)^{-1} r_h^2$, where $|\partial(T, \Omega_h)/\partial(M, J)|$ vanishes. If the same argument as in the case of black branes applies, black holes with $a > a_{crit}$ suffer from the Gregory Laflamme instability (See also Ref. [18]). Then, a_{crit} represents the maximal value below which the higher dimensional Kerr solution is adequate. Interestingly $a_{crit} < a_{max}$ (for $n = 2,\ 3,\ 4$ extra dimensions, $a_{crit} = 1.09,\ 1.07,\ 1.06$, whereas $a_{max} = 1.25,\ 1.89,\ 2.46$). Although it is widely believed that a dynamical instability exists, the value of a_{crit} obtained above is only heuristic. Thus, we consider two possible cases: the maximal value allowed for a is a_{crit} or a_{max}. A set of representative values for the parameter a is chosen as $a/a_{max} =$ 0.3, 0.5, 0.7, and $a/a_{crit} =$ 0.3, 0.5, 0.7. M is set to unity. Having fixed a in the above way, we compute the energy spectrum, shown in Fig. 1. We normalize the horizontal axis by using an effective temperature $T_{\rm eff}$ determined by fitting the data by a blackbody spectrum profile. The effective temperature $T_{\rm eff}$ is much higher than the Hawking temperature as shown in Fig. 2. However, the spectral shape is not so different from the thermal one except for the cases with $a \approx a_{max}$ (Fig. 1).

The renormalized spectra are enhanced for both lower and higher frequencies compared with the black body spectrum at $T = T_{\rm eff}$ (thick line). Except for very large values of a, the obtained spectra can be fit well by superpositions of black body profiles with width of about $2\Omega_H \times T_{\rm eff}$. The motion of the hypothetical emitting surface on the rotating black hole, relative to observers at infinity, causes the additional blueshift factor which varies from place to place. However, because of the change in the temperature and the rotation parameter during the evaporation, the broadening of the spectrum due to the rotation will not be identified straightforwardly. Wiggles can be seen in the spectrum for a small number of extra-dimensions, however, they are likely to disappear as T and a change during the evaporation. For high rotation velocity, the deviation from the thermal spectrum is much clearer. As a

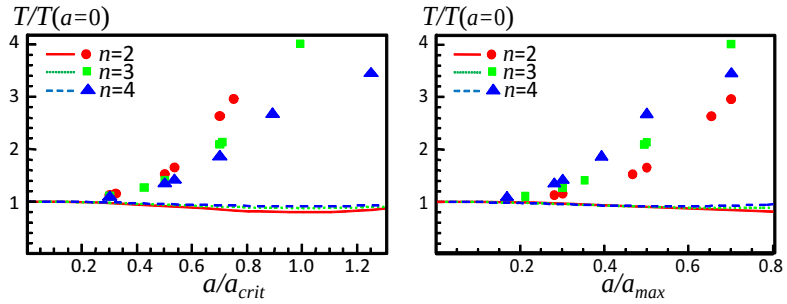

Figure 2: Effective Hawking temperature normalized by the temperature at $a = 0$ versus the rotation parameter a normalized by a_{crit} (left) and a_{max} (right).

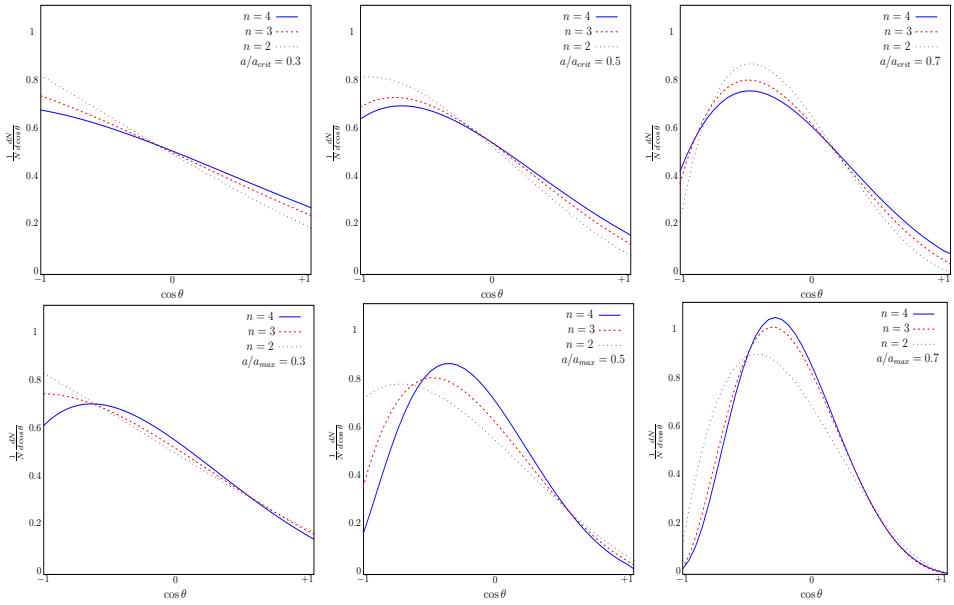

Figure 3: Angular distribution of emitted negative helicity fermions.

novel signature, we find that the spectrum is sharply cut off at high-frequencies for rapid rotation. This signature may survive even after taking into account the superposition of spectra along the evolutionary track of an evaporating micro black hole. This highly spinning regime is realized for $a > a_{crit}$.

In Fig. 3, the angular distribution of negative helicity particles is displayed for various parameters, setting ω to a representative frequency $\bar{\omega}$. The value $\bar{\omega}$ is chosen by requiring that the fraction of particles emitted with frequency below $\bar{\omega}$, $N(\bar{\omega}) = \int_0^{\bar{\omega}} dN$, to be 0.5.

The emission is suppressed in the direction anti-parallel to the black hole angular momentum. For rapid rotation, the particles tend to be emitted towards the equatorial plane. This concentration in the rapidly rotating case can also be seen in the helicity independent angular distribution [9]. The emission around both poles looks suppressed, but the observed apparent suppression is simply due to the large enhancement of emission in the directions close to the equatorial plane. The asymmetry in the helicity dependent angular distribution is visible even for relatively slow rotation and becomes evident as a increases. For very fast rotation, the concentration of the emitted particles around the equatorial plane may affect the features of cosmic ray air showers mediated by black holes.

For slow (rapid) rotation, the asymmetry decreases (increases) as n grows. This tendency may be used as an indicator to discriminate scenarios with different number of extra-dimensions. For a/a_{crit} fixed the peak position of the helicity dependent angular distribution is almost independent of n as shown in upper panel, Fig. 3. If we can align the direction of the axis of rotation of the black hole for various

events even approximately, we can collectively use the experimental data to achieve high statistics for the angular distribution of emitted particles. The LHC may allow to perform such measurements and for this reason it is important to estimate the error in the determination of the axis of rotation. A simple estimation can be perfomed by identifying the direction of the black hole angular momentum with the $l = 1$ (dipole) and $l = 2$ (quadrupole) moments (a more sophisticated statistical analyses may reduce the error). Assuming that the angular distribution shown in Fig. 3, the error δ in degrees, for 100 particles emitted, is summarized in Table 1.

a/a_{max}	0.3	0.5	0.7	a/a_{crit}	0.3	0.5	0.7
$n = 2$	18.20	15.17	9.47	$n = 2$	20.68	16.20	13.17
$n = 3$	19.93	13.43	8.19	$n = 3$	25.47	19.32	15.34
$n = 4$	20.03	10.97	7.50	$n = 4$	29.84	21.75	17.14

Table 1: Estimate of δ in degrees for the curves of fig. 3.

Acknowledgements. We acknowledge the support of the JSPS through Grants Nos. 19GS0219, 20740133, 17340075, 19540285 and 18204024, and Grant-in-Aid for the Global COE Program "The Next Generation of Physics, Spun from Universality and Emergence" from the Ministry of Education, Culture, Sports, Science and Technology (MEXT) of Japan. We thank Y. Sendouda for help with the numerics.

References

[1] T. Banks, W. Fischler, hep-th/9906038.

[2] S. Dimopoulos, G. Landsberg, Phys. Rev. Lett. **87** (2001) 161602.

[3] S. B. Giddings, S. Thomas, Phys. Rev. D**65** (2002) 056010.

[4] P.C. Argyres, S. Dimopoulos, J. March-Russell, Phys. Lett. B**441** (1998) 96.

[5] N. Arkani-Hamed, S. Dimopoulos, G. Dvali, Phys. Lett. B**429** (1998) 263.

[6] L. Randall, R. Sundrum, Phys. Rev. Lett. **83** (1999) 3370.

[7] D.M. Eardley, S.B. Giddings, Phys. Rev. D**66** (2002) 044011.

[8] H. Yoshino, Y. Nambu, Phys. Rev. D**66** (2002) 065004; Phys. Rev. D**67** (2003) 024009.

[9] D. Ida, K. Oda, S.C. Park, Phys. Rev. D**67** (2003) 064025; erratum *ibid.* D**69** (2004) 049901; Phys. Rev. D**71** (2005) 104039; Phys. Rev. D**73** (2006) 124022.

[10] G. Duffy, C. Harris, P. Kanti, E. Winstanley, JHEP **09** (2005) 049.

[11] M. Casals, S. Dolan, P. Kanti, E. Winstanley, JHEP **03** (2007) 019.

[12] R. Emparan, G.T. Horowitz, R.C. Myers, Phys. Rev. Lett. **85** (2000) 499.

[13] R. C. Myers and M. J. Perry, Ann. Phys. **172** (1986) 304.

[14] W. Unruh, Phys. Rev. Lett. **31** (1973) 1265; Phys. Rev. D**10** (1974) 3194.

[15] A. Vilenkin, Phys. Rev. Lett. **41** (1978) 1575; erratum *ibid.* **42** (1979) 195.

[16] W.H. Press, S.A. Teukolsky, The Astrophysical J. **185** (1973) 649.

[17] D. Page, Phys. Rev. D**14** (1976) 3260.

[18] R. Emparan, R.C. Myers, JHEP **09** (2003) 025.